JCTC Journal of Chemical Theory and Computation

Article

pubs.acs.org/JCTC

Hydration of Two Cisplatin Aqua-Derivatives Studied by Quantum Mechanics and Molecular Dynamics Simulations

Andrea Melchior,[†] Marilena Tolazzi,[†] José Manuel Martínez,[‡] Rafael R. Pappalardo,[‡] and Enrique Sánchez Marcos*[,‡]

[†]Department of Environmental and Physical Chemistry, University of Udine, 33100 Udine, Udine, Italy

[‡]Department of Physical Chemistry, University of Seville, 41012 Seville, Seville, Spain

Supporting Information

ABSTRACT: The hydration of the cisplatin aqua-derivatives, *cis*-$[PtCl(H_2O)(NH_3)_2]^+$ (w-cisplatin) and *cis*-$[Pt(H_2O)_2(NH_3)_2]^{2+}$ (w2-cisplatin), has been studied by means of classical molecular dynamics simulations. The new platinum complex-water interaction potential, w-cisplatin-W, has been built on the basis of the already obtained cisplatin-water interaction potential (cisplatin-W) [*J. Chem. Theory Comput.* **2013** *9*, 4562]. That potential has been then transferred to the w2-cisplatin-W potential. The w-cisplatin and w2-cisplatin atomic charges were specifically derived from their solute's wave functions. Bulk solvent effects on the complex-water interactions have been included by means of a continuum model. Classical MD simulations with 1 platinum complex and 1000 SPC/E water molecules have been carried out. Angle-solved radial distribution functions and spatial distribution functions have been used to provide detailed pictures of the local hydration structure around the ligands (water, chloride, and ammine) and the axial region. A novel definition of a multisite cavity has been employed to compute the hydration number of complexes in order to provide a consistent definition of their first-hydration shell. Interestingly, the hydration number decreases with the increase of the complex net charge from 27 for cisplatin to 23 and 18 for w-cisplatin and w2-cisplatin, respectively. In parallel to this hydration number behavior, the compactness of the hydration shell increases when going from the neutral complex, i.e. cisplatin, to the doubly charged complex, w2-cisplatin. Quantum mechanics estimation of the hydration energies for the platinum complexes allows the computation of the reaction energy for the first- and second-hydrolysis of cisplatin in water. The agreement with experimental data is satisfactory.

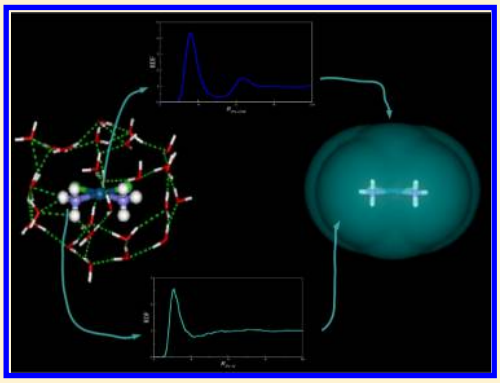

1. INTRODUCTION

The Pt(II) and Pd(II) aqua ions in aqueous solution display a square-planar arrangement of the ligands defining a plane containing the cation and an axial region. This asymmetry is expected to impose a hydration structure which no longer has a concentric sphere shape, as observed for tetrahedral and octahedral aqua ions, but characterized by two unlike regions: the equatorial and the axial one.[1] This feature of the Pt(II) and Pd(II) aqua ions stimulated numerous theoretical[2−9] and experimental studies[10−14] in the last years, especially focused on the precise description of the hydration structure and dynamics in the nonequatorial regions. Indeed, several works[4,6,8,11,14−17] evidenced the specific structural and dynamic properties of water in the axial region which was found to be markedly different from those of the first and the second shells. Besides the chemical interest of determining the hydration structure of Pt(II) and Pd(II) complexes, those studies have also been motivated by the relevance of such species in catalytic applications[18,19] and, as far as Pt(II) is concerned, for the pharmacological antitumoral activity of many platinum-based drugs.[20]

The most popular Pt(II)-based anticancer metallodrug, cisplatin ([*cis*-diammine- dichloroplatinum(II)]), has a two-stage action mechanism:[21] the first one is an intracellular activation by the hydrolysis of one chloride ligand to produce the monoaqua-derivative, *cis*-$[PtCl(H_2O)(NH_3)_2]^+$ (hereafter called "w-cisplatin"); in the second stage a relatively fast coordination of the w-cisplatin species to the DNA purine bases takes place followed by the hydrolysis of the second chloride and the formation of intrastrand cross-links. The result is a bent DNA that causes the cell death. It is known that for cisplatin and its active derivatives the first hydrolysis of one chloride is the rate-determining-step of the process leading to the coordination to DNA. Due to the relevance to the therapeutic function of platinum-based drugs, hydrolysis reactions have been the subject of a large number of theoretical studies aimed at correlating molecular factors to the observed kinetic and thermodynamic parameters.[22−31] In this framework, several studies[32−34] also evidenced the key role of explicit solvation in the theoretical description of the hydrolysis reaction rates for different platinum-based compounds and therefore the importance of a correct treatment of the hydration phenomenon of platinum-based anticancer drugs.

Received: November 1, 2014

DOI: 10.1021/ct500975a
J. Chem. Theory Comput. XXXX, XXX, XXX−XXX

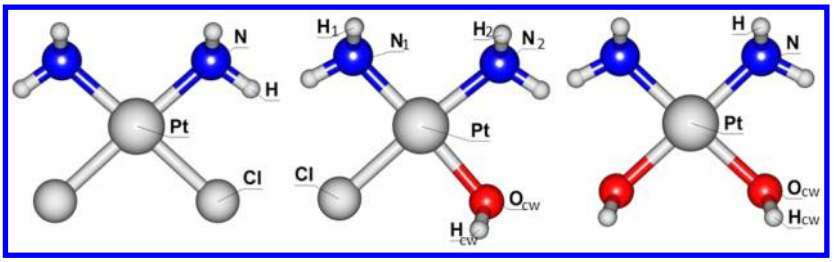

Figure 1. Atom types in cisplatin, w-cisplatin, and w2-cisplatin.

In a previous work[35] we studied the cisplatin hydration by means of classical molecular dynamics (MD), building a specific site−site cisplatin-water interaction potential (cisplatin-W) consisting of a Coulombic contribution and a series of r^{-n} terms (n = 4, 6, 8, 12). Coefficients were obtained by fitting about 4000 quantum-mechanical interaction energies of cisplatin-water dimers computed at the second-order Møller−Plesset perturbation theory level (MP2). This functional form was shown to be superior to the simpler 12−6 potential form in order to achieve a refined description of the cisplatin-water interactions in every region surrounding the complex. Furthermore, unlike previous studies on cisplatin,[36,37] the cisplatin-W potential was developed including the polarization induced by the solvent on the solute and the water molecule by a polarizable continuum model, to take into account many-body effects.

The hydrolyzed forms of cisplatin have received less attention, despite their role in the complex reaction scheme leading to the coordination to DNA.[20] Only in one work the structure and reactions of w-cisplatin and *cis*-$[Pt(NH_3)_2(H_2O)_2]^{2+}$ (hereafter called "w2-cisplatin") has been studied by ab initio MD and metadynamics.[33] However, although ab initio MD methods have the advantage of on-the-fly updating of the system wave function, they can only compute short simulation times and a reduced number of solvent molecules. This limits the phase space sampling and the physicochemical properties to be calculated. In this work, we develop a new first-principles based potential (hereafter "w-cisplatin-W") to describe the hydration of cisplatin aqua-derivatives on the basis of a classical scheme. This allows longer simulation times and larger system-sizes than in ab initio MD and could be also used in further QM/MM schemes. With the aim of reducing the effort in the potential development, a strategy based on the transferability of a part of the cisplatin-W potential[35] has been explored. Following the methodology of the previous cisplatin study, the fit of a relatively large number of ab initio interaction energies was performed to include the quantum-mechanical interaction in the water ligand region of the platinum complex. The transferability of this new potential to describe the hydration of the w2-cisplatin derivative has also been explored to provide a simple procedure to describe cisplatin derivatives in-solution by statistical methods.

2. METHODS

2.1. Potential Development. The strategy adopted to include the maximum information from the previous cisplatin-W potential[35] may be summarized in the following points:

- only the coefficients of the coordinated water molecule were optimized to best-fit the ab initio interaction energies in the w-cisplatin-H_2O dimers, freezing the previously obtained parameters for the other cisplatin centers, i.e. Pt, N, Cl, H;
- charges for the w-cisplatin complex were calculated using an electrostatic potential (ESP) fitting procedure, following the Merz−Kollman method;[38]
- the potential was validated by comparing the ab initio interaction energies with those calculated by the w-cisplatin-W potential for a series of dimers randomly sampled from a MD simulation containing the w-cisplatin complex;
- the w-cisplatin-W potential parameters were transferred to the w2-cisplatin-W potential, except for the charges which were recalculated with the ESP method.[38] The validation procedure was performed again for a series of dimers randomly sampled from a MD simulation containing the w2-cisplatin complex.

Geometry optimization of cisplatin aqua-derivatives and interaction energy calculations were carried out at the MP2 level. Platinum atom has been described by means of the Stuttgart-Dresden pseudopotentials,[39] while for the rest of the atoms 6-31+G(d,p) basis sets were employed. Two-body interaction energies were calculated using the SPC/E geometry[40] for water. As in the cisplatin case,[35] the new two-body potential (w-cisplatin-W) has been developed using the methodology proposed by Floris et al.[41,42] aimed at including solute−solvent interactions in the presence of a polarizable dielectric continuum. This strategy introduces the rest of the solvent as an isotropic dielectric medium surrounding the dimer (Pt(II) complex and H_2O). Interaction energies were corrected for the Basis Set Superposition Error (BSSE) by the counterpoise method (CP).[43] It is generally accepted that the full CP correction overestimates the BSSE,[44] and we previously proved for the cisplatin case[35] that 50% of the CP correction gives BSSE-corrected interaction energies comparable to those obtained with larger basis sets (aug-cc-pvTZ and aug-cc-pvQZ) but at a much lower computational cost. All calculations were performed with the Gaussian09 program.[45]

The functional form of the interaction potential used to fit the BSSE-corrected w-cisplatin-H_2O ab initio interaction energies was

$$V(r_{ij}) = \sum_{i}^{\text{w-cisplatin sites}} \sum_{j}^{\text{water sites}} \frac{C_{ij}^4}{r_{ij}^4} + \frac{C_{ij}^6}{r_{ij}^6} + \frac{C_{ij}^8}{r_{ij}^8} + \frac{C_{ij}^{12}}{r_{ij}^{12}} + \frac{q_i q_j}{r_{ij}} \quad (1)$$

The interaction energies of 1423 dimers were used to fit the C_{ij} parameters describing the interactions between the atoms of the water ligand (O_{cw} and H_{cw}) and the bulk water (OW and HW) in eq 1. The other terms, already obtained for cisplatin, were kept constant. Figure 1 shows the atom types defined in the complexes. Table S1 in the Supporting Information (SI) collects the parameter set.

The electrostatic part of the interaction is defined by charges calculated to fit to the electrostatic potential according to the

DOI: 10.1021/ct500975a
J. Chem. Theory Comput. XXXX, XXX, XXX−XXX

Merz–Kollman scheme.[38] Charges were calculated by fitting the electrostatic potential generated by the PCM polarized wave function and are given in Table S2 (SI). Because of the w-cisplatin asymmetry, the atoms of the two ammine ligands ($N_{1,2}$ and $H_{1,2}$ in Figure 1) were differentiated due to the different charges obtained by ESP fitting (Table S2 in the SI), but the same C_{ij} parameters as in the cisplatin-W potential were ascribed to both ammine ligands.

Only structures with attractive interaction energies, or repulsive ones smaller than +20 kcal mol^{-1}, were considered for the fitting. The final standard deviation (SD) of the fit is 1.43 kcal mol^{-1} (Figure S1(a) in the SI). To assess the reliability of the w-cisplatin-W potential, the interaction energies of 200 w-cisplatin-H_2O dimers, randomly sampled from a MD simulation, were calculated by the new potential and compared to the MP2 energies, the SD being 1.02 kcal mol^{-1}. Figure S1(b) in the SI shows the good linear correlation among the ab initio energies of the dimers and the values predicted by the developed potential.

The parameters obtained for the water ligand in the w-cisplatin-W potential (Table S1) were transferred to the w2-cisplatin-W potential for which only new ESP charges have been calculated (Table S2). The transferability of the potential parameters was checked as described above for 200 w2-cisplatin-H_2O dimers, randomly sampled from a MD simulation. A SD of 1.13 kcal mol^{-1} was obtained. Figure S1(c) in the SI shows the good behavior of the interaction energies predicted by the w2-cisplatin-W potential when compared to the MP2 ab initio energies of dimers.

2.2. Molecular Dynamics Simulations. Classical MD simulations were carried out with the DLPOLY program[46] modified in order to include eq 1 type potential. Platinum complexes have been placed in a cubic box and solvated with 1000 SPC/E water molecules.[40] The box length was adjusted to reproduce the water density of 0.997 g cm^{-3} at 298.15 K. Periodic boundary conditions were applied. The optimized geometries of w-cisplatin and w2-cisplatin were kept rigid during molecular dynamics simulations adopting the rigid unit algorithm. After an equilibration period of 100 ps, a simulation of 2.0 ns was run in the canonical ensemble (NVT) using a 1 fs time step. The Nosé–Hoover thermostat, with a time constant of 0.5 ps, was applied to keep the temperature at 298.15 K. The cutoff for the van der Waals interactions was 13.0 Å, and long-range electrostatic interactions were treated by the smooth particle mesh Ewald sum method.[47] The SHAKE algorithm was used to maintain the structure of the water molecule rigid. Atomic positions and velocities were saved every 100 steps for analysis.

3. RESULTS AND DISCUSSION

A first comparison of the behavior of the Pt complex-water interaction potentials can be displayed by examining the structures corresponding to the most favorable orientation of a water molecule with respect to each Pt complex. Figure 2 shows how the water molecule preference changes from ammine to water ligand when passing from the neutral complex (cisplatin), where the water molecule adopts a compromise between the two ammine groups and the metal cation, to the charged complexes (w-cisplatin and w2-cisplatin), where the water molecule forms a well-defined hydrogen bond with the water ligand. The interaction energies are −12.7, −20.2, and −25.4 kcal mol^{-1} for the cisplatin, w-cisplatin, and w2-cisplatin, respectively. It reflects both the increase of the electrostatic

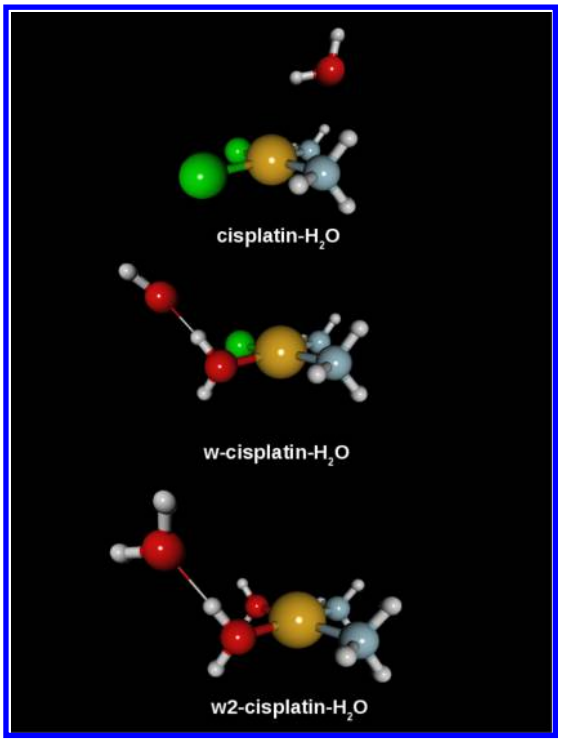

Figure 2. Minimum energy structure of the water molecule around the Pt complex for each interaction potential.

contribution with the net charge increase and the specific hydrogen bond interaction formed by the water ligand and the bulk water. Cisplatin-H_2O dimer is dominated by a compromise between the dipole–dipole interaction and the ammine group-water hydrogen bond.[35] The corresponding quantum-mechanical interaction energies computed for these geometries are −13.4 (cisplatin), −20.0 (w-cisplatin), and −25.3 (w2-cisplatin) kcal mol^{-1}, which support the good behavior of the developed potentials.

3.1. Thermochemistry of the Hydrolysis Processes of Cisplatin. Thermochemical data on the two successive hydrolysis processes provide relevant information to describe the equilibria involved in the cisplatin aquation:

$$cis\text{-}[PtCl_2(NH_3)_2] + H_2O \leftrightarrows cis\text{-}[PtClH_2O(NH_3)_2]^+ + Cl^- \quad (2)$$

$$cis\text{-}[PtClH_2O(NH_3)_2]^+ + H_2O \leftrightarrows cis\text{-}[Pt(H_2O)_2(NH_3)_2]^{2+} + Cl^- \quad (3)$$

Given that the development of the intermolecular potentials has involved quantum-mechanical calculations employing a continuum solvation model, the reaction energies in solution, ΔG_{sol} and ΔH_{sol}, can be evaluated as the sum of an intrinsic or gas phase (g.p.) contribution plus the solvation contribution (solv) by means of the following equations

$$\Delta G_{sol} = G_{sol}(\text{products}) - G_{sol}(\text{reactants}) = \Delta G_{g.p.} + \Delta\Delta G^{solv} \quad (4)$$

$$\Delta H_{sol} = H_{sol}(\text{products}) - H_{sol}(\text{reactants}) = \Delta H_{g.p.} + \Delta\Delta H^{solv} \quad (5)$$

DOI: 10.1021/ct500975a
J. Chem. Theory Comput. XXXX, XXX, XXX–XXX

Table 1. Energy Reactions (kcal/mol) for Cisplatin Hydrolysis Processes (2) and (3) in Gas Phase and Aqueous Solutions

		reaction					
		first hydrolysis (2)			second hydrolysis (3)		
		this work	Aono and Sakaki[a]	Zhang et al.[b]	this work	Aono and Sakaki[a]	Zhang et al.[b]
$\Delta E_{g.p.}$		115.8	104.5		212.9	202.0	
$\Delta H_{g.p.}$		118.1		123.5	214.3		214.3
$\Delta G_{g.p.}$		119.9		126.1	217.4		217.6
$\Delta H_{sol.}$	QM	3.6			4.3		
	exptal.[c]	1.8−2.8					
ΔG_{sol}	QM	6.4	7.5		8.1	11.7	
	exptal.[c,d,e]	3.5			5.0		
$\Delta\Delta H^{solv}$		−114.5			−210.3		
$\Delta\Delta G^{solv}$		−108.6	−97.0		−202.1	−190.3	

[a]Reference 59.

[b]Reference 29.

[c]Reference 56.

[d]Reference 57.

[e]Reference 58.

where

$$\Delta G_{g.p.} = G_{g.p.}(\text{products}) - G_{g.p.}(\text{reactants}) \quad (6)$$

$$\Delta\Delta G^{solv} = \Delta G^{solv}(\text{products}) - \Delta G^{solv}(\text{reactants}) \quad (7)$$

$$\Delta\Delta H^{solv} = \Delta H^{solv}(\text{products}) - \Delta H^{solv}(\text{reactants}) \quad (8)$$

$$\Delta H^{solv} = \Delta G^{solv} - T\Delta S^{solv} = \Delta G^{solv} + T\left(\frac{\partial \Delta G^{solv}}{\partial T}\right)_{P,V} \quad (9)$$

The cavity model definition provides the estimation of a solute solvation energy, ΔG^{solv}, which has a status of Gibbs energy.[48,49] Therefore, the correct way to proceed when dealing with in-solution reaction energies is to evaluate the thermal and entropic corrections to the 0 K internal energies derived from the quantum mechanical computations, as it was longly suggested by Pople's statistical formulation based on solute's structural parameters, masses, and vibrational frequencies.[50] From that, ΔG_{sol} values have been widely computed for many in-solution reactions.[49,51−54] A less usual procedure is that intended to evaluate the solvation enthalpy (ΔH^{solv}) using the continuum model. To achieve it, the solvation entropy (ΔS^{solv}) computation must be carried out within the continuum model. Tomasi et al.[55] proposed in the mid 1980s a method to compute the solvation entropy based on the classical thermodynamic relationship between S and G and the temperature dependence of the solvation Gibbs energy with the continuum model parameters: the cavity volume (V_{cav}) and the dielectric permittivity (ϵ). Thus

$$-\Delta S^{solv} = \left(\frac{\Delta G^{solv}}{\Delta \epsilon}\right)_{V_{cav}} \left(\frac{\partial \epsilon}{\partial T}\right)_{V_{cav}} + \left(\frac{\Delta G^{solv}}{\Delta V_{cav}}\right)_{\epsilon} \left(\frac{\partial V_{cav}}{\partial T}\right)_{\epsilon} \quad (10)$$

$((\Delta G^{solv})/(\Delta \epsilon))_{V_{cav}}$ and $((\Delta G^{solv})/(\Delta V_{cav}))_{\epsilon}$ being terms computed by finite differences by performing a few solvation energy computations of the solute where changes of V_{cav} or ϵ in the order of 1−2% of their reference values are carried out. For the temperature dependence of ϵ and V_{cav}, the water experimental values are taken. This clearly limits the application of this procedure to dilute solutions. Table 1 collects the evolution of the reaction energy from gas phase (g.p.) to aqueous solution (sol) for processes (**2**) and (**3**). Gas phase values for both reactions are highly endothermic, as expected with the monocation or dication derivative formation. The energy reaction change from internal energy to enthalpy and Gibbs energy is small, in the range of 3−5 kcal/mol, as also reported by Zhang et al.[29] On the contrary, solvation gives a major contribution to the thermochemical properties in aqueous solutions, as the calculated $\Delta\Delta G^{solv}$ and $\Delta\Delta H^{solv}$ values are of the same order of magnitude (but opposite sign) of the reaction energies in gas phase. In fact, it is running in an opposite direction to the gas phase trend. The process (**3**) is more endothermic in gas phase than (**2**) due to the formation of a divalent platinum complex. But it also has associated a greater stabilizing solvation energy mainly due to the Born term (ΔG^{solv}_{Born} is −49.1 and −198.1 kcal/mol for w-cisplatin and w2-cisplatin, respectively, and ΔG^{solv}_{Born} for the chloride is −83.0 kcal/mol). The reaction enthalpies and Gibbs energies in solution are values of a few kcal/mol, resulting from the cancellation of hundreds of kcal/mol of opposite sign corresponding to gas phase and solvation contributions. When comparing the solvation values in enthalpy versus Gibbs energy, it is observed that the gap is on the order of a few kcal/mol, being more negative the enthalpic solvation contribution. The reported experimental values have also been included for comparison in Table 1.[56−58] The agreement with the experimental values is satisfactory, although we should underline that such level of agreement is beyond the accuracy of the method employed.

Aono and Sakaki[59] have recently evaluated the reaction energies for the hydrolysis of *cis*- and *trans*-platin complexes undertaking a different approach based on the combined use of ab initio molecular orbital theory and liquid statistical theory (Reference Interaction Site model, RISM-SCF).[60,61] The general trend shown in Table 1 was already found by Aono and Sakaki. Bearing in mind the different methodology employed, the agreement is quite satisfactory. For instance, if we examine the values derived from their computations,[59] gas phase energy for reaction **2** is roughly 10 kcal/mol smaller than

DOI: 10.1021/ct500975a
J. Chem. Theory Comput. XXXX, XXX, XXX−XXX

ours (+104.5 kcal/mol vs +115.8 kcal/mol), but the solvation free energy contribution is also about 10 kcal/mol less negative than ours (−97.0 kcal/mol vs −108.6 kcal/mol). The combined results lead to these authors to predict +7.5 kcal/mol for the in-solution energy reaction of **2**, whereas our approach provides +6.4 kcal/mol. For reaction **3** the comparison of our results with those of Aono and Sakaki runs parallel to that found for reaction **2**, i.e., the gas phase result energy is +202 kcal/mol for them and +213 for us, whereas solvation contributions are −190.3 kcal/mol and −210 kcal/mol, respectively. Lau and Deubel,[32] following a quantum-mechanical strategy based on several continuum solvation models find values for ΔG_{sol} between +1 kcal/mol and +7 kcal/mol for the first hydrolysis reaction and +3 kcal/mol for the second one.

3.2. Hydration Structure: Radial Distribution Functions (RDF). The primary information to describe the hydration structure for these Pt-complexes is the examination of the Pt-OW and Pt-HW RDFs displayed at the top of Figure 3. Table 2 collects the main information for Pt-OW and Pt-HW RDFs. The first comparison shows that the Pt-OW RDFs for the aqua-derivatives are more similar between them than with that of cisplatin. As already discussed in our previous study,[35] the first broad peak for cisplatin (Figure 3(top) green line) contains several contributions resulting from the hydration of the different ligands surrounding the metal ion. Thus, although the maximum of this wide peak appears at 3.98 Å, it extends up to 6.0 Å that gives us a hydration number of 28 water molecules. This large number is not surprising if one bears in mind that it collects water molecules in a radius of 6 Å that roughly include the closest hydration environment for all ligands. When dealing with the aqua-derivatives, the first peak becomes more well-defined and compact (Figure 3(top), red and black lines). For the w-cisplatin (black line), the first-peak minimum is at 5.6 Å and the running coordination number goes down to 22.5, whereas for the w2-cisplatin (red line), the minimum appears at 5.2 Å and the coordinated water molecules go down to 18.5. The more compact hydration structure when increasing the platinum complex charge is also observed in the definition of a second peak centered at 6.5 Å for the w2-cisplatin, which becomes less intense at the same distance for the w-cisplatin and it is not present for the cisplatin. This indicates the presence of a second hydration shell in the aqua-derivatives, absent in the cisplatin.

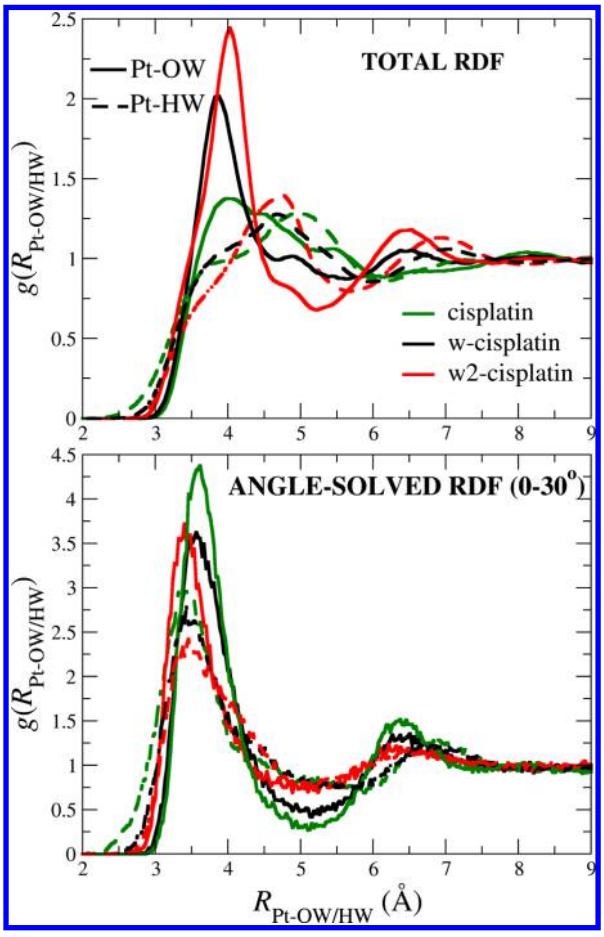

Figure 3. Pt-OW and Pt-HW RDFs for the cisplatin (taken from ref 35) and its two aqua-derivatives: global RDF (top) and angle-solved RDFs (bottom) for the axial region defined by the azimuthal angle 0° < θ < 30°.

Given the planar structure of the complexes, the regions above and below the molecular plane correspond to zones where water molecules could interact directly with the metal cation. As already presented in previous works[35,62] on complexes of similar symmetry, an angular decomposition of the total RDF is convenient to describe a particular region around the complex. Thus, the analysis of the axial hydration structure is carried out by means an angle-solved RDF[62] defined by the azimuthal angle θ which satisfies the condition 0° < θ < 30° above and below the molecular plane (see Figure S2 in the SI). Figure 3 (bottom) displays the Pt-OW and Pt-HW angle-solved RDFs for the three Pt(II) complexes. Previous experience dealing with axial regions has shown that a value for the azimuthal angle of 30° is a reasonable value to focus on this region, thus avoiding overlap between equatorial and axial regions.[4,6,14,35,62] In order to check this point for these complexes, angle-solved RDFs for the three Pt(II) complexes corresponding to narrower axial regions, i.e. 20° and 15° for the azimuthal angle, were extracted. They provide similar results to those presented in Figure 3 (bottom). The first remark is that angle-solved RDF pattern for the three complexes are much more similar among them than their corresponding total RDFs. The running coordination number is ca. 3 in all cases (see Table 2), the position of the first maximum of Pt-OW distributions decreasing from 3.61 Å (cisplatin), 3.56 Å (w-cisplatin) up to 3.39 Å (w2-cisplatin) when net charge increases in the complex. The second peak centered at 6.2−6.4 Å and containing about 5−6 oxygen atoms reflects the set of water molecules coordinating the axial ones of that region.

Regarding Pt-HW pairs, angle-solved RDF maxima for the first peak appear at almost the same values than those of Pt-OW RDFs, which indicates that in the axial region water molecules are parallel-orientated toward the platinum-containing plane rather than ion-dipole orientated. This is not surprising according to the mean distances adopted by the first-shell axial water molecules, ca. 3.5 Å which means that even for the doubly charged complex no *meso-shell* is formed, contrarily to that found in the cases of Pd(II) and Pt(II) aqua ions.[4−6,13−15,62−64] In the absence of a predominant driving-force, the axial regions become the result of three interaction contributions: the equatorial ligands, the net charge on the complex, and the condensed medium effects.

A detailed analysis of the hydration structure around the equatorial ligands may be obtained by examining the angle-

DOI: 10.1021/ct500975a
J. Chem. Theory Comput. XXXX, XXX, XXX−XXX

Table 2. Position of the First Peak (Å) and Running Coordination Number Derived from Total and Angle-Solved RDFs of the Main Pairs for Cisplatin, w-Cisplatin, and w2-Cisplatin

	cisplatin[a]			w-cisplatin			w2-cisplatin		
i-j pair	1st max.	1st min.	*n*	1st max.	1st min.	*n*	1st max.	1st min.	*n*
Pt-OW	3.98	6.0	28.	3.84	5.6	22.5	4.01	5.2	18.5
Pt-OW(0–30°)	3.61	5.2	2.9	3.56	5.2	2.9	3.39	5.2	3.0
Pt-HW	4.93	6.1	57.1	4.66	6.0	52.3	4.74	5.7	42.8
Pt-HW(0–30°)	3.40	5.2	7.	3.45	5.5	5.9	3.45	5.2	5.7
N-OW(0–90°)	3.14	4.3	5.	3.00	4.1	5.0	2.95	4.0	4.8
Cl-HW(0–90°)	3.29	4.1	11.5	3.29	4.1	11.3			
O-HW(0–90°)				3.18 (2.2)[b]	4.2 (2.8)[b]	11.1 (1.6)[b]	3.18	4.2	10.4
O-OW(0–90°)				2.57	3.7	4.7	2.54	3.8	4.5

[a]Values taken from ref 35.

[b]Data into parentheses corresponds to the initial plateau.

solved RDF centered on the most representative ligand atoms. Figure 4 presents the partial RDFs obtained by considering the volume of the external hemisphere centered at N, Cl, and O_{cw} atoms of ammonia, chloride, and water ligand, respectively. These hemispheres are defined by the solid Pt-X (X being N, Cl, or O_{cw}) angle $0° < \theta < 90°$, as shown in Figure S2 in the SI. Table 2 collects the main RDF data for their respective first peaks. A general comment rising from Figure 4 is that the water molecule arrangement around the equatorial ligands is quite similar among them, regardless of the platinum complex examined. This is particularly clear in the cases of chloride and ammine ligands (see top and bottom of Figure 4). When comparing the water ligand regions for w-cisplatin and w2-cisplatin some differences can be observed in both the O_{cw}-OW and O_{cw}-HW RDFs (middle of Figure 4). On one hand, the w2-cisplatin angle-solved O_{cw}-OW RDF appears to be more compact in its closest environment than that of the w-cisplatin. This may be in part due to the higher net charge of the w2-cisplatin complex. The largest difference appears in the angle-solved O_{cw}-HW RDFs, where a small plateau extends from 2.0 Å up to 2.8 Å in the case of the w-cisplatin, whereas a continuous increasing function appears for w2-cisplatin. From Table 2 it seems that roughly the plateau is associated with one water molecule hydrogen-bonded to the O_{cw} of the water ligand depicted in Figure 5a, because the tilt angle adopted by this molecule (~125°, see the w-cisplatin structure in Figure 1) favors an appropriate arrangement for the simultaneous interaction of this water molecule with the metal cation and three hydrogen bonds (HB) to three bulk water molecules, two as HB-donor and one as acceptor. In the case of the doubly charged complex, the more important electrostatic contribution causes an alignment of the two ligand water molecules closer to the ion-dipole-like interaction (tilt angle is ~140°, see w2-cisplatin in Figure 1) preventing a closer coordination of bulk water molecules to their oxygen atoms (Figure 5b) and the formation of a HB as proton acceptor. Given that our Pt complex model is rigid one could ascribe this differential result to an overstructured solvent. A definite answer to this question may only be given by the development of a flexible model for the metal complexes. Nevertheless, we have carried out additional quantum-mechanical and MD calculations for w-cisplatin and w2-cisplatin considering other conformations in order to get a deeper insight into this issue. For w-cisplatin we have checked that there is another conformational isomer involving the water ligand with an orientation *anti* with respect to the chloride (tilt angle ~220°). The energy of this isomer is about 3 kT higher than that of the isomer *syn* here studied (see Figure 1). The energy barrier for the conformer interconversion is about 5 kT. This leads to expect the structural prevalence of the *syn* isomer in solution for the w-cisplatin complex. In the case of the w2-cisplatin complex, the *syn-anti* energy barrier is ~3 kT, and the isomer energy gap is 2.5 kT. This means that the isomer examined should be the most representative

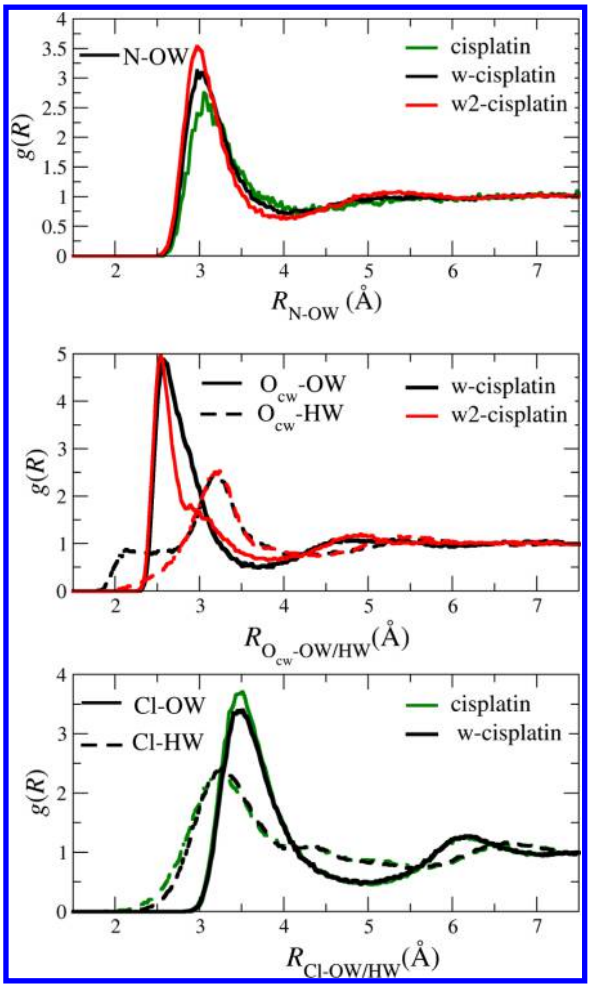

Figure 4. Angle-solved RDFs corresponding to the solid angle $0° < \theta < 90°$ around the corresponding X-OW or X-HW line for the cisplatin (taken from ref 35) and its two aqua-derivatives: N-OW (top), O_{cw}-OW and O_{cw}-HW (medium), and, Cl-OW and Cl-HW (bottom).

DOI: 10.1021/ct500975a
J. Chem. Theory Comput. XXXX, XXX, XXX−XXX

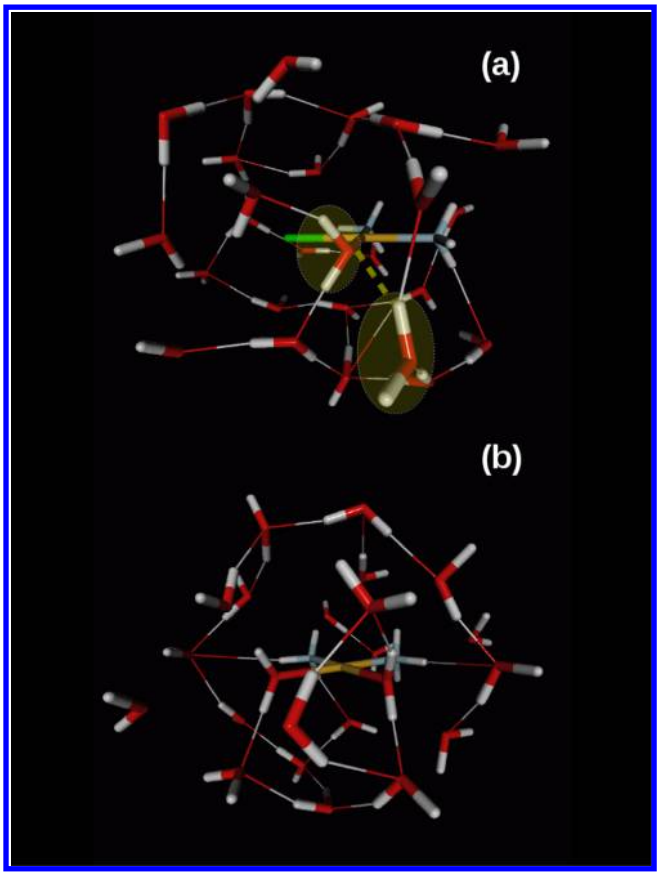

Figure 5. Snapshots showing the water environment for w-cisplatin (a) and w2-cisplatin (b) complexes. Bulk water molecule interacting with the water ligand in w-cisplatin as HB donor is emphasized.

structure in solution. An MD simulation of the *anti* isomer of w-cisplatin also shows the small plateau in the O_{cw}-HW RDFs. Contrarily, an MD simulation of the w-cisplatin with the same value of the tilt angle for the water ligand than that adopted by the w2-cisplatin complex leads to an O_{cw}-HW RDF where no plateau at a short distance is observed. This seems to confirm that the formation of the H-donating HB is intimately joined to a certain degree of pyramidalization of the water ligand in the complex.

The difficulty in supporting the structural analysis of the hydration on the basis of total RDFs may be recognized by examining Figure 6, where the total and the angle-solved N-OW RDFs for the two ammino groups of the w-cisplatin complex are shown separately. It must be recalled that in the w-cisplatin case, both ammine ligands are no longer symmetric as shown in Figure 1. Figure 6 shows that both of the two angle-solved N_1-OW and N_2-OW RDFs (dotted lines) are quite similar for the two ammine ligands, but the total $N_{1/2}$-OW RDFs present a shifting of about 0.7 Å at the position of the second peak (second-peak maxima are at 5.0 and 5.7 Å for N_2-OW and N_1-OW, respectively). This differential structural behavior is the consequence of the different region scanned by the two types of RDFs. In the case of the total (conventional) ones, at distances beyond the first neighbors, the hydration environment of other ligands, such as chloride or water, starts being shared by ammine ligands (see Figure S2 in the SI) and then the appearing of peaks at different distances in N_1-OW and N_2-OW RDFs. On the contrary, when dealing with the 0–90° angle-solved RDFs centered on the N_1 or N_2 atom, the

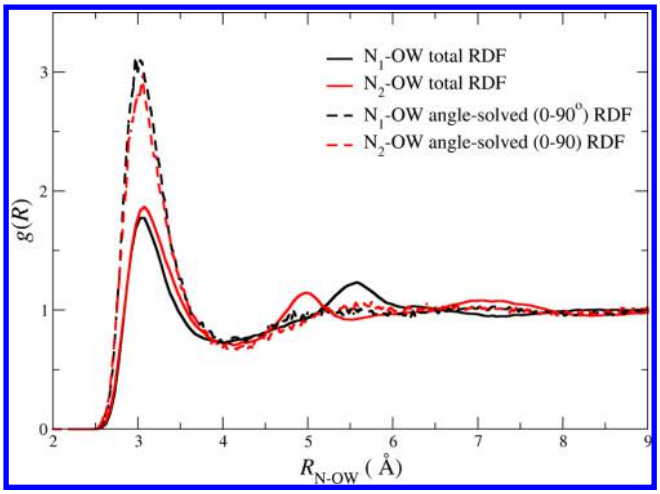

Figure 6. Angle-solved vs total RDFs of the two N-OW pairs in the w-cisplatin complex.

scanned region is essentially that belonging to the ammine ligands.

3.3. Hydration Structure: Spatial Distribution Functions. Spatial distribution functions (SDF) give a 3D-view of the hydration structure around each platinum complex. Isosurfaces for oxygen (red) and hydrogen (white) atoms have been built for probability values 2.5 times greater than those of the average solvent density. An axial and an equatorial view have been displayed in Figure for the three complexes. To make easier the comparison among them, the plot of difference SDF (ΔSDF) between each aqua-derivative and the cisplatin have also been included in the figure. The examination of the axial view sequence from cisplatin to w2-cisplatin shows that the main changes appear on the left hemispheres, the complex region where both chloride ligands are replaced by water molecules. The water region in w-cisplatin located two solvent molecules hydrogen bonded to the water ligand. These are responsible of the white lobe in w-cisplatin and the two white lobes close to water ligands of w2-cisplatin. The ΔSDF plots for w-cisplatin−cisplatin and w2-cisplatin−cisplatin show that these white lobes are enclosing red lobes, closer to the water ligands. This increase of water-solvent oxygen atom probability is a consequence of the well-defined hydrogen bonds formed with the water ligands as HB acceptors. The other significant difference observed in the ΔSDF (w-cisplatin-cisplatin) plot is a banana-like red lobe in between the water ligand and the ammine ligand. This increase of probability is due to the well-defined hydrogen bond promoted by the tilted water molecule in the complex, which was first noted by the plateau of the O-HW RDF in Figure 4(middle). When looking at the same region in the ΔSDF (w2-cisplatin-cisplatin) case, the feature is less marked, as was also observed in the corresponding O-HW RDF in Figure 4(middle). The right hemisphere corresponding to the ammine ligands does not change significantly as well as the platinum axial regions neither change. It is only observed a slight increase of hydrogen atom density of the hydration water bonded to the ammine ligands as a consequence of the slight acid character of the ammine hydrogen atoms of w-cisplatin and w2-cisplatin complexes due to the cation nature of them (cf. ESP charges in Table S2).

The SDF sequence examined from the equatorial view completes the description of the hydration distribution. The visual impact of more expanded white regions when passing

DOI: 10.1021/ct500975a
J. Chem. Theory Comput. XXXX, XXX, XXX−XXX

from cisplatin to w2-cisplatin SDFs is a direct indication of the more orientated and more spatially restricted hydration water molecules. Thus, the well-defined red and white lobes close to the hydrogen atoms of the water ligands in the w2-cisplatin on the left side of its SDF equatorial view is a clear display of the hydrogen bond formed with bulk water molecules. This is also clearly present in the difference SDF. The w-cisplatin SDF as well as its corresponding ΔSDF shows this pattern of a double red-white lobe in the close environment of the water ligand hydrogen atoms (left plot on the bottom of equatorial view). This figure also allows the visualization of a white lobe surrounded by a triangle-shaped red lobe (see left-bottom plot in the equatorial view frame), which corresponds to the hydrogen bond formed by the water ligand oxygen atom and the bulk water already visualized in the axial view. Only the red lobe corresponding to the oxygen atoms is appreciated by perspective reasons in the intermediate region between the water and the ammine in the axial view of Figure 7 (ΔSDF(w-cisplatin−cisplatin) in the axial frame). This is again consistent with the plateau of the w-cisplatin O-HW RDF appearing between 2 and 2.8 Å in Figure 4 (medium). Interestingly for the w2-cisplatin case there is not such well-defined triangle-shape lobes, and its corresponding angle-solved RDF exhibits a monotone increasing instead of a plateau.

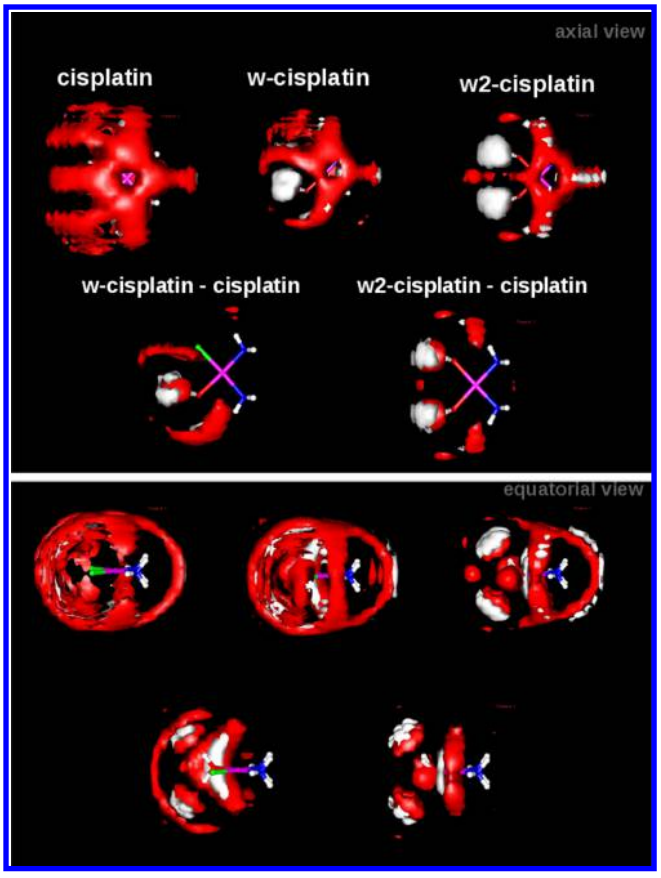

Figure 7. Axial (top) and equatorial (bottom) views of SDF (isosurface value is 2.5 times the average solvent density) for oxygen (red) and hydrogen (white) atoms calculated for the cisplatin and its aqua-derivatives (top of the frames). SDF difference (bottom of the frames) for each aqua-derivative with respect to the cisplatin complex.

3.4. Hydration Numbers on the Basis of a Multisite Definition Cavity. One of the most characteristic solvation datum is the number of solvent molecules surrounding the solute: *the solvation number*. When dealing with single ions the running integration number associated with the monatomic Ion-S (S being the most representative solvent atom) RDF is usually employed.[1,65,66] However, for metal complexes, such as those here considered, radial topology is lost and makes more difficult and ambiguous the meaning of the solvation number based on a Copernican view of the problem. In our previous in-solution cisplatin study[35] we proposed the computation of a hydration number based on the counting of water molecules inside a multisite cavity defined by the overlap of spheres centered on the metal cation and the main ligand atoms, i.e., N (ammine ligand), Cl, and O_{cw} (water ligand). Figure S3 in the SI displays a sketch of the multisite cavity definition, where it is shown how from the atomistic MD simulation, the angle-solved RDFs extracted from the trajectory are used to define the different spheres surrounding the main ligand atoms, this way allowing the definition of the region belonging to the hydration shell. Their corresponding sphere radii are taken from the first minimum of the angle-solved RDF for the various centers of the complex except platinum for which a more restricted value was adopted in order to avoid double-counting of shared water molecules with the equatorial ligands. The hydration numbers obtained from the multisite cavities are collected in Table 3 together with the radii used for each atom. It is worth pointing out that the radii values are common for the three platinum complexes. The hydration number reduces when going from the neutral complex, cisplatin (27), to the singly charged w-cisplatin (23) and to the doubly charged w2-cisplatin (18), as expected from the increasing complex-water interactions promoting the compactness of the hydration shell. For the sake of comparison, Table 3 collects the different hydration numbers obtained on the basis of the total Pt-OW RDFs shown in Figure 3 which would represent the usual way to proceed in estimating this property. Due to the RDF complexity, there is not a clear minimum to define the first hydration shell, then Table 3 gives tentative values which might have been assigned to the possible minimum radii considered as the first shell limit. The most ambiguous case is that of cisplatin where three values could be chosen, but for both of the two aqua-derivatives there

Table 3. Hydration Numbers of the Different Pt(II) Complexes Obtained by Different Methods and Distribution of Water Molecules among Regions Belonging to Different Ligands

	molecule					
	cisplatin[a]		w-cisplatin		w2-cisplatin	
method	n	r_{min} (Å)	n	r_{min} (Å)	n	r_{min} (Å)
multisite cavity	27	*b*	23.4	*b*	17.6	*b*
total Pt-OW RDF	8.5	4.5	12.7	4.7	13.5	4.6
	17.3	5.1	22.5	5.6	18.5	5.2
	28.5	6.0				
molecules in 1-region	55%		20%		35%	
molecules in 2-regions	35%		47%		28%	
molecules in 3-regions	10%		33%		35%	

[a]Taken from ref 35. [b]Values adopted for the multisite cavity r_c(Pt-OW) = 3.9 Å, r_c(N-OW) = 4.1 Å, r_c(Cl-OW) = 4.9 Å, r_c(O_{cw}-OW) = 3.7 Å.

DOI: 10.1021/ct500975a
J. Chem. Theory Comput. XXXX, XXX, XXX−XXX

are two options, one at short distances (~4.7 Å for w-cisplatin and 4.6 Å for w2-cisplatin, see Figure 3 top) and another at longer distances (~5.6 Å for w-cisplatin and 5.2 Å for w2-cisplatin). This way the hydration description for a given complex may change significantly. Contrarily, the hydration number estimation based on the multisite cavity appears as a much more robust definition to provide consistent values for nonradial arrangements. A final remark on this method to estimate the hydration number of platinum complexes is associated with the potential aim of decomposing the hydration number in ligand contributions. This is to say, how many first-shell water molecules can be associated with an individual ligand? Our experience leads to conclude that it is not possible to answer this question because the high level of overlap among the ligand environment regions. This can be quantified by collecting the first-shell water molecules which are located in only 1-ligand sphere or 2-ligand spheres or more. Table 3 shows that in the best case, i.e. that of cisplatin, only one-half of the water molecules can be labeled as hydrating only one ligand. The worst case is that of w-cisplatin where only one-fifth of them could be associated with only one ligand.

4. CONCLUSIONS

This work has shown an efficient procedure to develop solute−solvent intermolecular potentials for the aqua-derivatives of the cisplatin complex involved in its aquation processes. The procedure established for building the new potential has proven the transferability of the nonelectrostatic terms associated with the common centers of all complexes, i.e. Pt, N, and Cl. The new ingredients are the charges associated with the different sites and the nonelectrostatic terms of the water molecules present in the complexes. The comparison among the ab initio optimized structures and those derived from the classical potentials lead to a noticeable agreement that makes confident the ulterior classical MD simulations carried out with these intermolecular potentials. The methodology presented opens the way to further extension toward square-planar complexes containing other transition metal complexes,[67] as well as to improved interaction potentials by including the polarizable character of the water model and the metal complexes and their molecular flexibility.

The analysis of the complex hydration cannot be based on usual RDFs only, due to the different hydration pattern of the ligands around the central platinum cation. Angle-solved RDFs as well as SDFs have proven to give a more refined hydration structure view. Water molecules in the complexes appear to be the ligands defining a more compact hydration structure in their close environment. On the basis of the previous information, a new hydration number associated with a multisite cavity volume supplies a more precise and unambiguous quantitative estimation of what is the cisplatin-derivative hydration number. The hydration structure of the series of cisplatin complexes shows a clear trend to be more compact and well-defined when going from the cisplatin to the w2-cisplatin, as well as to decrease their hydration number, 27 for cisplatin, 23 for w-cisplatin, and 18 for w2-cisplatin.

The reaction energies associated with the hydrolysis processes in solution have been pretty well quantified in solution by means of the PCM continuum model, including the less usual enthalpy estimation. This is in part due to the ability of the molecular shape of the cavity, which in part collects specific interactions on different solute regions, as already pointed out by Tomasi et al.[68] It is remarkable that theoretical reaction energies in solution diverges less than a 10% from the experimental results. Nevertheless, the hydration structure and the specific components of the solvation play an important role in the ligand exchange mechanism, and its theoretical estimation would need the inclusion of a detailed molecular description of solvent molecules. We believe that the new intermolecular potentials here presented will certainly contribute to describe the involved reaction mechanism of the cisplatin and its derivatives in biological media.

■ ASSOCIATED CONTENT

Ⓢ Supporting Information

Tables including fitted coefficients and ESP charges for the different metal complexes. Plots of the fitted vs ab initio interaction energies for the w-cisplatin-W potential and comparison between the MP2 interaction energies of dimers randomly sampled from MD simulations containing w-cisplatin or w2-cisplatin. Sketch showing the ligand region defined for the angle-solved RDFs plotted in Figures 3 and 4. Sketch showing the definition of the multisite cavity. This material is available free of charge via the Internet at http://pubs.acs.org.

■ AUTHOR INFORMATION

Corresponding Author

*Phone: 34 955421008. E-mail: sanchez@us.es.

Notes

The authors declare no competing financial interest.

■ ACKNOWLEDGMENTS

We thank the Spanish Ministerio de Economia y Competitividad for financial support (project number CTQ2011-25932). A.M. and M.T. also thank the Italian Ministry of Education, University and Research (MIUR, project PRIN NANOMED, # 2010FPTBSH).

■ REFERENCES

(1) Richens, D. T. *The Chemistry of Aqua Ions*; John Wiley: Chichester, 1997; Chapter 10.
(2) Ayala, R.; Sánchez Marcos, E.; Diaz-Moreno, S.; Sole, V. A.; Muñoz Paez, A. *J. Phys. Chem. B* **2001**, *105*, 7588−7593.
(3) Naidoo, K. J.; Klatt, G.; Koch, K. R.; Robinson, D. J. *Inorg. Chem.* **2002**, *41*, 1845−1849.
(4) Martínez, J. M.; Torrico, F.; Pappalardo, R. R.; Sánchez Marcos, E. *J. Phys. Chem. B* **2004**, *108*, 15851−15855.
(5) Hofer, T. S.; Randolf, B. R.; Shah, S.; Rode, B. M.; Persson, I. *Chem. Phys. Lett.* **2007**, *445*, 193−197.
(6) Torrico, F.; Pappalardo, R. R.; Sánchez Marcos, E.; Martínez, J. M. *Theor. Chem. Acc.* **2006**, *115*, 196−203.
(7) Beret, E. C.; Pappalardo, R. R.; Doltsinis, N. L.; Marx, D.; Sánchez Marcos, E. *ChemPhysChem* **2008**, *9*, 237−240.
(8) Kozelka, J.; Bergès, J.; Attias, R.; Fraitag, J. *Angew. Chem., Int. Ed.* **2000**, *39*, 198−201.
(9) Vidossich, P.; Ortuño, M.; Ujaque, G.; Lledós, A. *ChemPhysChem* **2011**, *12*, 1666−1668.
(10) Beret, E. C.; Provost, K.; Mueller, D.; Sánchez Marcos, E. *J. Phys. Chem. B* **2009**, *113*, 12343−12352.
(11) Rizzato, S.; Bergés, J.; Mason, S.; Albinati, A.; Kozelka, J. *Angew. Chem., Int. Ed.* **2010**, *49*, 7440−7443.
(12) Truflandier, L. A.; Autschbach, J. *J. Am. Chem. Soc.* **2010**, *132*, 3472−3483.
(13) Truflandier, L. A.; Sutter, K.; Autschbach, J. *Inorg. Chem.* **2011**, *50*, 1723−1732.
(14) Bowron, D. T.; Beret, E. C.; Martín-Zamora, E.; Soper, A. K.; Sánchez Marcos, E. *J. Am. Chem. Soc.* **2012**, *134*, 962−967.

DOI: 10.1021/ct500975a
J. Chem. Theory Comput. XXXX, XXX, XXX−XXX

(15) Purans, B. J.; Fourest, B.; Cannes, C.; Sladkov, V.; David, F.; Venault, L.; Lecomte, M. *J. Phys. Chem. B* **2005**, *109*, 11074−11082.
(16) Beret, E. C.; Pappalardo, R. R.; Marx, D.; Sánchez Marcos, E. *ChemPhysChem* **2009**, *10*, 1044−1052.
(17) Hofer, T. S.; Randolf, B. R.; Rode, B. M.; Persson, I. *Dalton Trans.* **2009**, 1512−1515.
(18) Leininger, S.; Olenyuk, B.; Stang, P. J. *Chem. Rev.* **2000**, *100*, 853−907.
(19) Tílvez, E.; Menéndez, M. I.; López, R. *Inorg. Chem.* **2013**, *52*, 7541−7549.
(20) Jamieson, E. R.; Lippard, S. J. *Chem. Rev.* **1999**, *99*, 2467−2498.
(21) Kelland, L. *Nat. Rev. Cancer* **2007**, *7*, 573−584.
(22) Zimmermann, T.; Leszczynski, J.; Burda, J. V. *J. Mol. Model.* **2011**, *17*, 2385−2393.
(23) Burda, J. V.; Zeizinger, M.; Leszczynski, J. *J. Chem. Phys.* **2004**, *120*, 1253−1262.
(24) Deubel, D. V. *J. Am. Chem. Soc.* **2004**, *126*, 5999−6004.
(25) Deubel, D. V. *J. Am. Chem. Soc.* **2006**, *128*, 1654−1663.
(26) Pavelka, M.; Lucas, M. F. A.; Russo, N. *Chem.—Eur. J.* **2007**, *13*, 10108−10116.
(27) Lucas, M. F. A.; Pavelka, M.; Alberto, M. E.; Russo, N. *J. Phys. Chem. B* **2009**, *113*, 831−838.
(28) Alberto, M. E.; Lucas, M. F. A.; Pavelka, M.; Russo, N. *J. Phys. Chem. B* **2009**, *113*, 14473−14479.
(29) Zhang, Y.; Guo, Z.; You, X.-Z. *J. Am. Chem. Soc.* **2001**, *123*, 9378−9387.
(30) Alberto, M. E.; Butera, V.; Russo, N. *Inorg. Chem.* **2011**, *50*, 6965−6971.
(31) Alberto, M. E.; Russo, N. *Chem. Commun.* **2011**, *47*, 887−889.
(32) Lau, J. K.-C.; Deubel, D. V. J. *J. Chem. Theory Comput.* **2006**, *2*, 103−106.
(33) Lau, J. K.-C.; Ensing, B. *Phys. Chem. Chem. Phys.* **2010**, *12*, 10348−10355.
(34) Melchior, A.; Sánchez Marcos, E.; R. Pappalardo, R.; Martínez, J. M. *Theor. Chem. Acc.* **2011**, *128*, 627−638.
(35) Melchior, A.; Martínez, J. M.; Pappalardo, R. R.; Sánchez Marcos, E. *J. Chem. Theory Comput.* **2013**, *9*, 4562−4573.
(36) Lopes, J. F.; de A. Menezes, V. S.; Duarte, H. A. A.; Rocha, W. R.; De Almeida, W. B.; Dos Santos, H. A. F. *J. Phys. Chem. B* **2006**, *110*, 12047−12054.
(37) Fu, C.-F.; Tian, S. X. *J. Chem. Phys.* **2010**, *132*, 174507.
(38) Besler, B. H.; Merz, K. M.; Kollman, P. A. *J. Comput. Chem.* **1990**, *11*, 431−439.
(39) Andrae, D.; Häussermann, U.; Dolg, M.; Stoll, H.; Preuss, H. *Theor. Chim. Acta* **1990**, *77*, 123−141.
(40) Berendsen, H. J. C.; Grigera, J. R.; Straatsma, T. P. J. *J. Phys. Chem.* **1987**, *91*, 6269−6271.
(41) Floris, F.; Persico, M.; Tani, A.; Tomasi, J. *Chem. Phys. Lett.* **1992**, *199*, 518−524.
(42) Floris, F. M.; Martínez, J. M.; Tomasi, J. *J. Chem. Phys.* **2002**, *116*, 5448−5459.
(43) Boys, S.; Bernardi, F. *Mol. Phys.* **1970**, *19*, 553−566.
(44) Kim, K. S.; Tarakeshwar, P.; Lee, J. Y. *Chem. Rev.* **2000**, *100*, 4145−4185.
(45) Frisch, M. J.; Trucks, G. W.; Schlegel, H. B.; Scuseria, G. E.; Robb, M. A.; Cheeseman, J. R.; Scalmani, G.; Barone, V.; Mennucci, B.; Petersson, G. A.; Nakatsuji, H.; Caricato, M.; Li, X.; Hratchian, H. P.; Izmaylov, A. F.; Bloino, J.; Zheng, G.; Sonnenberg, J. L.; Hada, M.; Ehara, M.; Toyota, K.; Fukuda, R.; Hasegawa, J.; Ishida, M.; Nakajima, T.; Honda, Y.; Kitao, O.; Nakai, H.; Vreven, T.; Montgomery, J. A., Jr.; Peralta, J. E.; Ogliaro, F.; Bearpark, M.; Heyd, J. J.; Brothers, E.; Kudin, K. N.; Staroverov, V. N.; Kobayashi, R.; Normand, J.; Raghavachari, K.; Rendell, A.; Burant, J. C.; Iyengar, S. S.; Tomasi, J.; Cossi, M.; Rega, N.; Millam, J. M.; Klene, M.; Knox, J. E.; Cross, J. B.; Bakken, V.; Adamo, C.; Jaramillo, J.; Gomperts, R.; Stratmann, R. E.; Yazyev, O.; Austin, A. J.; Cammi, R.; Pomelli, C.; Ochterski, J. W.; Martin, R. L.; Morokuma, K.; Zakrzewski, V. G.; Voth, G. A.; Salvador, P.; Dannenberg, J. J.; Dapprich, S.; Daniels, A. D.; Farkas, O.; Foresman, J. B.; Ortiz, J. V.; Cioslowski, J.; Fox, D. J. *Gaussian09 Revision C.01*.
(46) Smith, W.; Yong, C. W.; Rodger, P. M. *Mol. Simul.* **2002**, *28*, 385−471.
(47) Frenkel, D., Smit, B. *Understanding molecular simulation: from algorithms to applications*, 2nd ed.; Academic Press: Harcourt, FL, 2002; Chapter 12.
(48) Rivail, J., Rinaldi, D. In *Computational Chemistry, Review of Current Trends*; Leszczynski, J., Ed.; World Scientific: New York, 1996; Vol. *1*, Chapter 4.
(49) Tomasi, J.; Persico, M. *Chem. Rev.* **1994**, *94*, 2027−2094.
(50) Hehre, W. J.; Radom, L.; Schleyer, P.; Pople, J. A. *Ab Initio Molecular Orbital Theory*; Wiley: New York, 1986; pp 226−260.
(51) Sánchez Marcos, E.; Pappalardo, R. R.; Rinaldi, D. *J. Phys. Chem.* **1991**, *95*, 8928−8932.
(52) Tomasi, J.; Mennucci, B.; Cammi, R. *Chem. Rev.* **2005**, *105*, 2999−3093.
(53) Cramer, C. *Essentials of Computational Chemistry*; John Wiley & Sons: Chichester, 2004; Chapter 11.
(54) Kelly, C.; Cramer, C. J.; Truhlar, D. G. J. *J. Chem. Theory Comput.* **2005**, *1*, 1133−1152.
(55) Bonacorsi, R.; Palla, P.; Tomasi, J. *J. Am. Chem. Soc.* **1984**, *106*, 1945−1950.
(56) Miller, S.; House, D. A. *Inorg. Chim. Acta* **1991**, *187*, 125−132.
(57) Perumareddi, J. R.; Adamson, A. W. *J. Phys. Chem.* **1968**, *72*, 414−420.
(58) Coe, J. S. *MTP Int. Rev. Sci.: Inorg. Chem., Ser.* **1974**, *2*, 45.
(59) Aono, S.; Sakaki, S. *J. Phys. Chem. B* **2012**, *116*, 13045−13062.
(60) Chandler, D.; Anderson, H. *J. Chem. Phys.* **1972**, *57*, 1930−1931.
(61) Hirata, F.; Rossky, P. *Chem. Phys. Lett.* **1981**, *83*, 1930−1931.
(62) Beret, E. C.; Martínez, J. M.; Pappalardo, R. R.; Sánchez Marcos, E.; Doltsinis, N. L.; Marx, D. *J. Chem. Theory Comput.* **2008**, *4*, 2108−2121.
(63) Jalilehvand, F.; Laffin, L. *Inorg. Chem.* **2008**, *47*, 3248−3254.
(64) Sutter, K.; Truflandier, L. A.; Autschbach, J. *ChemPhysChem* **2011**, *12*, 1448−1455.
(65) Marcus, Y. *Ion Solvation*; Wiley: Chichester, 1985; Chapter 4.
(66) Ohtaki, H.; Radnai, T. *Chem. Rev.* **1993**, *93*, 1157−1204.
(67) Alberto, M. E.; Cosentino, C.; Russo, N. *Struct. Chem.* **2012**, *23*, 831−839.
(68) Martínez, J.; Pappalardo, R. R.; Sánchez Marcos, E.; Mennucci, B.; Tomasi, J. *J. Phys. Chem. B* **2002**, *106*, 1118−1123.

DOI: 10.1021/ct500975a
J. Chem. Theory Comput. XXXX, XXX, XXX−XXX